Title

Specific heat and sound velocity at the relevant competing phase of high-temperature superconductors

Journal

Proceedings of the National Academy of Sciences of the United States of America, 112(20)

ISSN

0027-8424

Authors

Varma, Chandra M

Zhu, Lijun

Publication Date

2015-05-19

DOI

10.1073/pnas.1417150112

Peer reviewed

Specific heat and sound velocity at the relevant competing phase of high-temperature superconductors

Chandra M. Varma[1] and Lijun Zhu[1]

Department of Physics and Astronomy, University of California, Riverside, CA 92521

Edited by Zachary Fisk, University of California, Irvine, CA, and approved April 6, 2015 (received for review September 4, 2014)

Recent highly accurate sound velocity measurements reveal a phase transition to a competing phase in $YBa_2Cu_3O_{6+\delta}$ that is not identified in available specific heat measurements. We show that this signature is consistent with the universality class of the loop current-ordered state when the free-energy reduction is similar to the superconducting condensation energy, due to the anomalous fluctuation region of such a transition. We also compare the measured specific heat with some usual types of transitions, which are observed at lower temperatures in some cuprates, and find that the upper limit of the energy reduction due to them is about 1/40th the superconducting condensation energy.

high-temperature superconductor | pseudogap | thermodynamics | resonant ultrasound spectroscopy | loop current order

A significant step forward toward understanding high-temperature superconductivity is the variety of experimental results that have led to the widespread acceptance of the idea (1) that a phase with a broken symmetry competes with superconductivity in the underdoped region, often called the pseudogap region. There are a plethora of suggested phases (2–15). However, experimental results (16) consistent with transition to only one of them are observed at the pseudogap temperature T^*, where major changes in transport and thermodynamics occur in all cuprates. Charge density waves (CDWs) are observed in some compounds at lower temperatures. The idea that a broken symmetry phase competes with superconductivity makes thermodynamic sense only if the energy gained due to it is comparable to that gained through the superconducting transition in their coexistence region. The energy gained is related to the specific heat associated with the transition. Extraordinarily, however, no specific heat signature of a phase transition has been identified in the available measurements at the pseudogap temperature T^*. The much more accurately measured sound velocity singularity near the transition temperature is proportional to the heat capacity and can be used to find the symmetry class of the phase transition. In this paper, we use the recent highly accurate sound velocity measurements (17) and the best available specific heat measurements in $YBa_2Cu_3O_{6+\delta}$ (18–20) to show that phase transitions to the universality class of the loop current-ordered state with free-energy reduction similar to the measured superconducting condensation are consistent with the sound velocity and with lack of identifiable observation in the specific heat.

Sound velocity changes near a phase transition, as shown below, are proportional to $-\gamma(T) = -C_v/T$, where C_v is the specific heat, if the transition temperature depends linearly on the strain. Since they are measured with a factor of $O(10^{-2})$ greater accuracy than the deductions from the best available specific heat measurements, they can be used to decipher the universality class to which the transition at T^* belongs and therefore their specific heat. The free-energy reduction can be calculated from the specific heat expected for the class of broken symmetry and its magnitude.

The free energy due to a phase transition at temperature T_x is a homogeneous function of $(T - T_x)$. The elastic constants of a solid are given by the second derivative of the free energy with respect to the relevant strain. Therefore, the isothermal sound velocity variation δc_λ in a polarization λ associated with the phase transition, normalized to the background smoothly varying sound velocity $c_{0\lambda}$ for $\delta c_\lambda \ll c_{0\lambda}$, is given by

$$\frac{\delta c_\lambda(T-T_x)}{c_{0\lambda}} = \frac{1}{2\rho c_{0\lambda}^2}\left[-\frac{C_v(T-T_x)}{T}\left(\frac{dT_x}{du_\lambda}\right)^2 + S(T-T_x)\frac{d^2T_x}{du_\lambda^2}\right]. \quad [1]$$

$C_v(T-T_x)$ and $S(T-T_x)$ are the specific heat at constant volume and entropy associated with the part of the free energy associated with the transition at T_x, i.e., the part that is a homogeneous function of $(T-T_x)$. Here ρ is the density. In mean field phase transitions, such as the superconducting transition, this reduces to the relation commonly used. Noting that the second contribution above is much smoother than the first and typically $(1/T_x)\left(\frac{dT_x}{du_\lambda}\right)^2$ is similar or larger than $\frac{d^2T_x}{du_\lambda^2}$, we need to consider only the first term. Comparing the sound velocity variations at two different transitions, one at T_c and the other at T^*,

$$\frac{\delta c_\lambda(T-T^*)}{\delta c_\lambda(T-T_c)} = \frac{C_v(T-T^*)}{C_v(T-T_c)}\left(\frac{dT^*/du_\lambda}{dT_c/du_\lambda}\right)^2. \quad [2]$$

Results

Transitions to the Loop-Ordered State. Changes in sound velocity, consistent in their location in the phase diagram with the previous observations both of T_c and T^*, have been measured (17) at two dopings in very high-quality samples of $YBa_2Cu_3O_{6+\delta}$. The results for the larger doping, $\delta = 0.98$, which is close to the peak of the superconducting transition temperature, and close to

Significance

A variety of experiments have supported the idea that high-temperature superconductivity is caused by the interaction of quantum mechanical zero-point fluctuations of a competing order with electrons. One of the strangest features of this order is that a transition to it appears to occur without a noticeable specific heat anomaly. We show unambiguously that a proposed order, in which currents spontaneously flow in close loops within each unit cell of the compound, is such that an unusual signature of transition to it is found in the sound velocity experiments but that it is unobservable in the specific heat measurements. Stringent conditions are provided by the analysis for other possible orders to be relevant to the fundamental physics of high-temperature superconductivity.

Author contributions: C.M.V. designed research; C.M.V. and L.Z. performed research; L.Z. analyzed data; and C.M.V. and L.Z. wrote the paper.

The authors declare no conflict of interest.

This article is a PNAS Direct Submission.

[1]To whom correspondence may be addressed. Email: chandra.varma@ucr.edu or lijun.zhu@ucr.edu.

This article contains supporting information online at www.pnas.org/lookup/suppl/doi:10.1073/pnas.1417150112/-/DCSupplemental.

the putative quantum critical point, are particularly interesting since the multiplicative factor in Eq. **1** is amplified near the quantum critical point. Fig. 1 gives the measured change in relative frequency for three different modes, or, equivalently, the relative change in the sound velocity as a function of temperature (17) showing both the superconducting transition and a transition at about 68 K consistent with the continuation of the loop current order transition seen through polarized neutron scattering (16). The Fig. 1 *Insets* give, on a different scale, the signature of the superconducting transition and the pseudogap transition after subtracting the background signal. It is noteworthy that the width of the transition at the *d*-wave superconducting transition at T_c is measured to be less than about 0.1 K (17), giving a ratio of width to the transition temperature of $O(10^{-3})$, whereas the same ratio is larger than $O(1)$ at the lower transition.

Consider the thermodynamic properties of the loop current order transition. This broken symmetry, with which many varieties of experimental results (16, 17, 21–26) are consistent, is in the statistical mechanical class of the Ashkin–Teller (AT) model that does not have a specific heat divergence, but singularities exist in the order parameter as a function of temperature. The asymptotically exact critical exponents were derived by Baxter (27); over the range of the parameters for the AT model consistent with the symmetry of the observed phase, the specific heat exponent varies from 0 to −2. The specific heat as a function of temperature (and the order parameter) was calculated (28) by Monte Carlo methods on asymptotically large lattices and is given for two sets of parameters in Fig. 2. In the *Lower Inset* of Fig. 1, the sharpest of the observed sound velocity changes near $T^* \approx 68K$ is plotted together with the prediction from the AT model for these two sets of parameters. These parameters were chosen among those calculated (28) to be such as to give, using Eq. **1**, a sound velocity signature similar to those observed. Note that the two theoretical curves shown bound the region of parameters that reproduce the sound velocity variations, and note the striking similarity between the measurements and the calculations with regard to the wide fluctuation regime for transitions of this universality class.

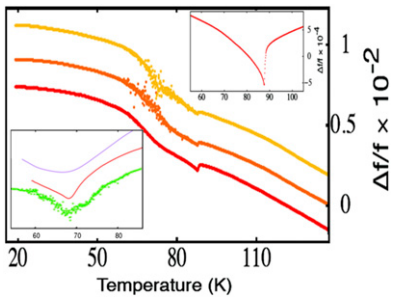

Fig. 1. The temperature variation of the relative frequency changes or sound velocity changes measured by Shekhter et al., taken from figure 2b. Reprinted by permission from Macmillan Publishers Ltd from ref. 17. Three different modes are shown with the vertical axis displaced. *Upper* and *Lower Insets* show amplified regions near the superconducting and pseudogap transitions with smooth background subtracted, taken from figures 1c and 4c (green curve), respectively. Reprinted by permission from Macmillan Publishers Ltd from ref. 17. The temperature dependence of the variation in sound velocity for the AT model, using Eq. **1** for two different sets of parameters in Fig. 2, is also shown (*Lower Inset*); the three curves are mutually displaced. To obtain these results from the dimensionless temperature scale in Fig. 2, the peaks are made to coincide with the experimental transition temperature of about 68 K and with a multiplicative factor for the vertical scale required by Eq. **1**. Note the sharpness of the signature of the superconducting transition in the sound velocity and the wide fluctuation region at the lower transition, which is reproduced by the two theoretical curves that bound the parameters needed to fit the experimental results.

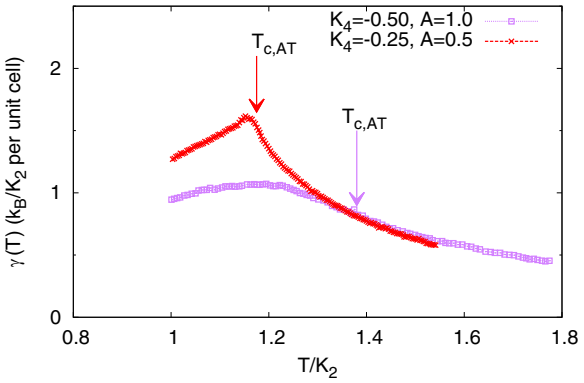

Fig. 2. The exactly calculated specific heat coefficient $\gamma(T)$ for the Ashkin–Teller model for two different values of the parameters from Grönsleth et al. (28). The temperature scale is normalized to the parameter K_2 of the AT model. The transition temperature in terms of this scale is given in ref. 28 and is close to but does not coincide with the peak of the specific heat, but marks the singularity of the order parameter. The vertical scale in the figure is such that the asymptotic high-temperature entropy, $S(T) = \int_0^T dT'\gamma(T')$, for all of the curves is k_B ln 4/unit cell, corresponding to a model of four unit vectors per unit cell.

Having thus approximately fixed the parameters of the AT model, we calculate the specific heat quantitatively to compare with the observations. The free-energy reduction due to the transition(s) is calculated from the measured specific heat (18–20) (see *Calculations of the Condensation Energy* for details). The value obtained is 52.7 joules per mole. The calculated specific heat for the AT model (28) shown in Fig. 2 is for the four discrete states of the AT model with one classical spin 1 per unit cell, so that the asymptotic entropy at high temperatures in every case is k_B ln 4 per unit cell. We must determine the value of the effective spin for the ordered state. As in any transition in which the relevant free energy is drawn to collective degrees of freedom from that of itinerant Fermions, this can be an arbitrary number. However, if the transition is as significant thermodynamically as the superconducting transition, we can determine it by calculating the reduction in energy due to it to approximately equal the superconducting condensation energy. The procedure is also described in *Calculations of the Condensation Energy*. With this constraint, $\gamma(T)$ for the two sets of parameters of the AT model is plotted together with the experimental $\gamma(T)$ in Fig. 3. We present also the measured value minus the calculated $\gamma(T)$. It is obvious due to the wide fluctuation region that it is not possible to tell from the specific heat that there is a phase transition near 68 K, which is visible in the sound velocity measurement. This is even without taking into account the process of deduction of the electronic contribution to the specific heat and the error bars in the specific heat measurements.

The electronic specific heat for $YBa_2Cu_3O_{6+\delta}$, at various δ, has been deduced by subtracting the measured value from that of samples with partial substitution of Cu by Zn (18–20). The Zn-doped samples are not superconducting and have almost the same lattice-specific heat. Unfortunately, as is now known, independently, from Knight shift (29), optical conductivity (30), and neutron scattering (31) measurements, the pseudogap properties are observed in the Zn-doped samples starting at the same $T^*(x)$ as without Zn doping, albeit rounded compared with the pure Cu samples. Therefore, although subtraction of the specific heat measurements of Zn-doped samples is an excellent way to deduce the change in electronic heat capacity due to superconductivity, it is not helpful in providing information about the details of thermodynamics near the pseudogap temperature.

We note that the peaks of $\gamma(T)$ in the two theoretical curves in Fig. 3 are 6.1 millijoules per (mol K^2) and 4.1 millijoules per

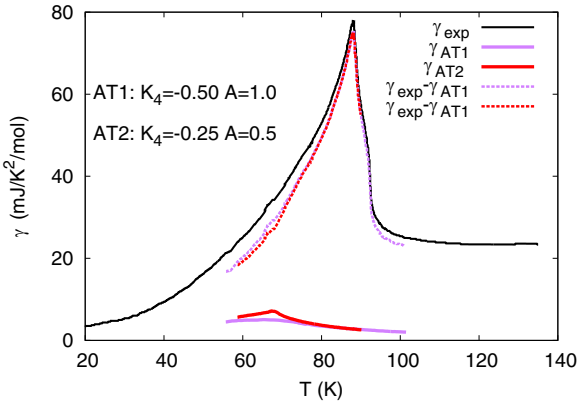

Fig. 3. Comparison between the measured $\gamma(T)$ from Cooper et al. (20) and $\gamma(T)$ calculated for the AT model with two sets of parameters. The latter have the same condensation energy as the superconducting condensation energy. Also shown are their differences, $\gamma_{exp} - \gamma_{AT}$, providing an estimation of $\gamma(T)$ if there were superconducting transition only. The physics of why the small $\gamma(T)$ of the AT model gives the same condensation energy as the mean field superconducting condensation energy is easily understood from the wide and relatively smooth fluctuation regime of its entropy and the fact that the specific heat is related to the derivatives of the entropy (see *Calculations of the Condensation Energy* for details).

(mol K^2), a factor of 6 and 9 below the deduced value, respectively. The width of the peak at half height is about 40 K. Besides the point made in the last paragraph, we can try to estimate what error is allowed in an absolute measurement of the specific heat as a function of temperature to see this specific heat feature. Given the width of the specific heat feature in the pure limit, one finds that an uncertainty in determining $\gamma(T)$ of about 0.5 millijoules per (mol K^2) would be the limiting error for the smoother of the two sets of parameters to be decipherable.

It should be mentioned that a broad bump in the specific heat of the magnitude expected from the AT model is directly observed (32) (without making any subtractions) for La_{2-x} Sr_xCuO_4, systematically decreasing to lower temperature as doping is increased and invisible above $x = 0.22$. The error bars in these measurements were not specified. Ultrasound anomalies, besides those at the superconducting transition temperature, in this compound, as well as those in $YBa_2Cu_3O_{6+\delta}$ with a $T_c \approx 85K$ at what we would now call $T^* \approx 120K$, albeit not so clear-cut as the latest measurements, were seen long ago (33).

Let us return now to Eq. **2** to estimate the relative factors of variation of the transition temperatures with strain. From Fig. 3, the peak height of $\gamma(T)$ at near T^* may be taken to be about a factor of 8 smaller than the peak height of $\gamma(T)$ near T_c. The maximum value of the ultrasound anomaly $(\Delta f/f)$ of Fig. 1 has a typical value of 7×10^{-4} at T_c, while that around T^* has a maximum value above background of 1.2×10^{-3} (17). Using Eq. **2**, one concludes that dT^*/du_λ should be about 4 times larger than dT_c/du_λ. The modes are mixtures of different polarizations for each of which we do not have separate information. We only know that the volume of the crystal changes linearly with δ and that near the quantum critical point $dT^*/d\delta \gg dT_c/d\delta$. Thus the estimates made here are quite reasonable, at least for the bulk modulus components of the sound velocity.

Transitions to Other Ordered States. Let us now consider some of the other transitions that have been reported in the cuprates (6–8, 34, 35) in relation to the specific heat expected due to them for a given free-energy reduction. Some of the transitions are being reported in underdoped cuprates at various temperatures through high-quality measurements in NMR (34), neutron scattering (35), elastic and inelastic X-ray scattering (6–8), and ultrasound measurements as a function of a magnetic field (36). Let us confine ourselves to those at zero magnetic field. The first important point is that no phase transition other than the time reversal breaking order, consistent in its symmetry with the loop current order, has ever been reported near the onset of the pseudogap. Nevertheless, the upper limits on the free-energy reduction due to transitions to other ordered states may be placed from the symmetry class of the phase transition and the lack of observation of a specific heat signature. Detailed sound velocity measurements, which have been made so far only for a small number of samples, would be even more effective in discerning different proposed orders. Let us specifically consider transitions of the incommensurate charge density wave type and compare the observations to those in the well-studied electronically highly anisotropic material 2H-$TaSe_2$. The energy reduction due to the second-order charge density wave transition at about 120 K is measured to be about 67 joules per mole (37), only about 15% larger than the energy reduction due to superconductivity in $YBa_2Cu_3O_{6.9}$. We plot the measured $\gamma(T)$ due to the transition taken from figure 3 of ref. 37 scaled to half the measured condensation energy in $YBa_2Cu_3O_{6+\delta}$ also in Fig. 4 at the transition temperature of 2H-$TaSe_2$. It is clear that a structural transition of this type with about (1/40) of the condensation energy of the superconducting transition would be easily visible in the specific heat measurements if it were to occur at 120 K; a smaller fraction of condensation energy would be detectable at lower temperatures. Sound velocity features of a transition, presumably a CDW, are clearly seen in $YBa_2Cu_3O_{6.67}$ (36), but only for fields larger than about 20 teslas and temperature greater than about 40 K. A CDW has been observed through both hard and soft X-rays at $\delta \approx 0.67$ with a magnitude of lattice distortion increasing with a magnetic field and estimated to be 10^{-3} a at 17 teslas, while, in $TaSe_2$, the distortion is $3 \times 10^{-2}a$, a being the nearest neighbor lattice constant. In underdoped Hg cuprates, which show quantum oscillations above about 50 teslas, the magnitude and correlation length of the CDW in zero field is at least an order of magnitude less (38) than in $YBa_2Cu_3O_{6.67}$. In $YBa_2Cu_4O_8$, which also shows quantum oscillations above about 50 teslas, no CDW distortions are visible at zero field, using the same methods as those that show them in $YBa_2Cu_3O_{6.67}$.

If the energy gain due to other transitions is much less than the superconducting condensation energy, they may be regarded as phenomena incidental to the principal remarkable features of the phase diagram of cuprates, which are all extravagant in spending the free energy. As mentioned, a variety of charge stripe/checkerboard phases (2–12, 14, 15) with varying support in experiments have been discussed without their magnitudes from which the energy reduction may be estimated. They are all of the Ising/CDW variety discussed in relation to Fig. 3. An exceptional

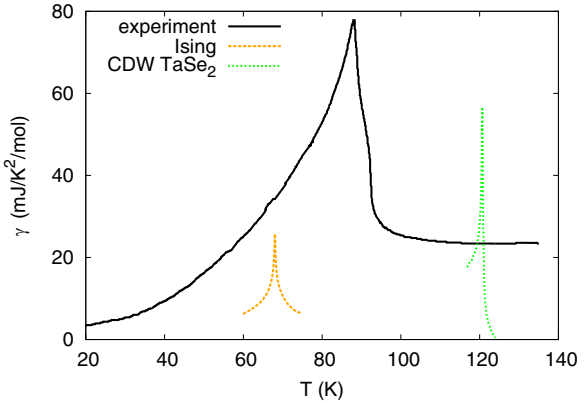

Fig. 4. Comparison between the measured $\gamma(T)$ from Cooper et al. (20) and $\gamma(T)$ calculated for the 2D Ising model, and 2H-$TaSe_2$ with CDW transition (37).

case is the intraunit cell $\mathbf{Q}=0$ charge order (14, 15) of $d_{x^2-y^2}$ symmetry deduced by two very refined experiments. If this order parameter were to occur independently, it would also belong to the Ising class and could be ruled as irrelevant. However, such a distortion has been shown (39) by symmetry considerations to be mandated in the loop current-ordered state and to be proportional to the modulus square of the loop order parameter. We suggest further experiments to study the temperature dependence of the distortion to check whether this occurs together with loop current order. If so, and if they are of small magnitude, the charge density observations of this class (15), the direct observations of the loop current order (16) and its manifestations in a variety of other experiments (21–26), the specific heat (18, 19), and the sound velocity (17) are all mutually consistent.

Discussion

To summarize, we have shown that the sound velocity and specific heat measurements can be used to discern the broken symmetry phase in high-temperature superconductors. We have found the universality class of the loop current-ordered phase is consistent with the experimental observation that the reduction of free energy of the transition captured from the sound velocity measurements is not identifiable in specific heat measurements. We have also analyzed other types of transitions and shown that the reduction of free energy for these transitions can only be up to about 1/40 the superconducting condensation energy to be in consistent with the experiments.

We discuss now whether it is possible that the relative width of the ultrasound signatures at the superconducting transition and at the pseudogap transition shown in Fig. 1 may be due to disorder, rather than due to the intrinsic difference between the universality class of the superconducting transition and the loop order transition in the pure limit. This is a legitimate question since, as mentioned, the variation of $T^*(\delta)$ with δ is much larger than that of $T_c(\delta)$ at the δ of the sample for which the data are shown in Fig. 1. Therefore, sample inhomogeneities will have a much bigger effect on the variations in $T^*(\delta)$ within the sample than in $T_c(\delta)$. We have estimated in a self-consistent argument above in comparing the magnitudes of the sound velocity signatures, for the same free-energy reductions, that $(dT^*/d\delta)\approx 4(dT_c/d\delta)$. Therefore the relative broadening of the transition, if of similar universality class, should be only about a factor of 4 larger, whereas, in fact, it is about 10^3 larger. One may also directly get an estimate of the mean free path due to disorder in the sample from the microwave conductivity and from the relative width of the superconducting d-wave transition, for which nonmagnetic impurities are also pair breaking. Knowing that the superconducting correlation length $\xi\approx 1.6$ nm, one estimates the mean free path to be $\ell\approx\xi(T_c/\delta T_c)\approx 1.6$ μm. This is consistent with the estimate from the microwave conductivity measurements (40), which give about 4 μm. For samples of this purity, broadening of any transition due to disorder of $O(1)$ can occur only if $(dT^*/d\delta)\approx 10^3(dT_c/d\delta)$. This is unreasonable. Moreover, using the thermodynamic result of Eq. **1**, this would give orders of magnitude larger sound velocity anomaly at its peak than observed for the same total free-energy reduction as superconductivity.

We should mention that consistency of specific heat and sound velocity has not been proven here for the specific model of loop current order, only for a statistical model to which the loop current order belongs. We have ruled out classes of order of the Ising kind, irrespective of the details of the microscopic model underlying it. Commensurate CDWs belong to this class. For the transition at $T^*(x)$, they are unnecessary to discuss, since no such transition is found at that temperature (41). Our result, however, encompasses that when they are observed in spectroscopic experiments at lower temperatures, bounds can be put on the free-energy reduction due to them by lack of a signature either in the specific heat measurement or an ultrasound measurement at fields below about 20 teslas.

Finally, the difficulty of the loop current model—that in the pure limit, it does not give a gap—should be mentioned. This issue has been addressed by showing that small angle scattering due to pinned domain walls between different orientations of loop current order, due to defects, gives the observed features of a pseudogap (42). Some experiments have been suggested to test this conclusion and to see if the ideas and calculations are valid.

ACKNOWLEDGMENTS. We thank Albert Migliori, Cyril Proust, Brad Ramshaw, and Arkady Shekhter for discussions of the sound velocity measurements. Discussions with Nevin Barišić, Philippe Bourges, Martin Greven, Marc-Henri Jullien, and Suchitra Sebatian were very helpful. This research was supported by National Science Foundation Grant DMR 1206298.

1. Varma CM (1997) Non-fermi-liquid states and pairing instability of a general model of copper oxide metals. *Phys Rev B* 55(21):14554–14580.
2. Comin R, et al. (2014) The symmetry of charge order in cuprates. arXiv:1402.5415.
3. Tranquada J, et al. (1996) Neutron-scattering study of stripe-phase order of holes and spins in $La_{1.48}$ $Nd_{0.4}$ $Sr_{0.12}$ Cuo_4. *Phys Rev B* 54(10):7489–7499.
4. Kim YJ, Gu G, Gog T, Casa D (2008) X-ray scattering study of charge density waves in La_{2-x} Ba_xCuo_4. *Phys Rev B* 77(6):064520.
5. Chang J, et al. (2012) Direct observation of competition between superconductivity and charge density wave order in YBa_2 Cu_3 $O_{6.67}$. *Nat Phys* 8(12):871–876.
6. Ghiringhelli G, et al. (2012) Long-range incommensurate charge fluctuations in (Y,Nd) $Ba_2Cu_3O_{6+x}$. *Science* 337(6096):821–825.
7. Bakr M, et al. (2013) Lattice dynamical signature of charge density wave formation in underdoped YBa_2 Cu_3 O_{6+x}. *Phys Rev B* 88(21):214517.
8. da Silva Neto EH, et al. (2014) Ubiquitous interplay between charge ordering and high-temperature superconductivity in cuprates. *Science* 343(6169):393–396.
9. Achkar AJ, et al. (2012) Distinct charge orders in the planes and chains of ortho-III-ordered $YBa_2Cu_3O_{6+\delta}$ superconductors identified by resonant elastic x-ray scattering. *Phys Rev Lett* 109(16):167001.
10. Torchinsky DH, Mahmood F, Bollinger AT, Božović I, Gedik N (2013) Fluctuating charge-density waves in a cuprate superconductor. *Nat Mater* 12(5):387–391.
11. Hoffman JE, et al. (2002) A four unit cell periodic pattern of quasi-particle states surrounding vortex cores in $Bi_2Sr_2CaCu_2O_{8+\delta}$. *Science* 295(5554):466–469.
12. Li JX, Wu CQ, Lee DH (2006) Checkerboard charge density wave and pseudogap of high-Tc cuprate. *Phys Rev B* 74(18):184515.
13. Simon ME, Varma CM (2002) Detection and implications of a time-reversal breaking state in underdoped cuprates. *Phys Rev Lett* 89(24):247003.
14. Fujita K, et al. (2014) Simultaneous transitions in cuprate momentum-space topology and electronic symmetry breaking. *Science* 344(6184):612–616.
15. Fujita K, et al. (2014) Direct phase-sensitive identification of a *d*-form factor density wave in underdoped cuprates. *Proc Natl Acad Sci USA* 111(30):E3026–E3032.
16. Bourges P, Sidis Y (2011) Novel magnetic order in the pseudogap state of high- copper oxides superconductors. *C R Phys* 12(5-6):461–479.
17. Shekhter A, et al. (2013) Bounding the pseudogap with a line of phase transitions in $YBa_2Cu_3O_{6+\delta}$. *Nature* 498(7452):75–77.
18. Loram J, Luo J, Cooper J, Liang W, Tallon J (2001) Evidence on the pseudogap and condensate from the electronic specific heat. *J Phys Chem Solids* 62(1-2):59–64.
19. Loram JW, Mirza KA, Cooper JR, Liang WY (1993) Electronic specific heat of $YBa_2Cu_3O_{6+x}$ from 1.8 to 300 K. *Phys Rev Lett* 71(11):1740–1743.
20. Cooper JR, Loram JW, Kokanović I, Storey JG, Tallon JL (2014) The pseudogap in YBa_2 Cu_3 $O_{6+\delta}$ is not bounded by a line of phase transitions: Thermodynamic evidence *Phys Rev B* 89(20):201104(R).
21. Li Y, et al. (2011) Magnetic order in the pseudogap phase of $HgBa_2$ $CuO_{4+\delta}$ studied by spin-polarized neutron diffraction. *Phys Rev B* 84(22):224508.
22. Xia J, et al. (2008) Polar Kerr-effect measurements of the high-temperature $YBa_2Cu_3O_{6+x}$ superconductor: Evidence for broken symmetry near the pseudogap temperature. *Phys Rev Lett* 100(12):127002.
23. He RH, et al. (2011) From a single-band metal to a high-temperature superconductor via two thermal phase transitions. *Science* 331(6024):1579–1583.
24. Leridon B, Monod P, Colson D, Forget A (2009) Thermodynamic signature of a phase transition in the pseudogap phase of YBa_2 Cu_3 O_x high-T_c superconductor. *EPL* 87(1):17011.
25. Kaminski A, et al. (2002) Spontaneous breaking of time-reversal symmetry in the pseudogap state of a high-T_c superconductor. *Nature* 416(6881):610–613.
26. Lubashevsky Y, Pan L, Kirzhner T, Koren G, Armitage NP (2014) Optical birefringence and dichroism of cuprate superconductors in the THz regime. *Phys Rev Lett* 112(14): 147001.
27. Baxter RJ (1982) *Exactly Solved Models in Statistical Mechanics* (Academic, London).
28. Grönsleth MS, et al. (2009) Thermodynamic properties near the onset of loop-current order in high-T_c superconducting cuprates. *Phys Rev B* 79(9):094506.
29. Alloul H, Mendels P, Casalta H, Marucco JF, Arabski J (1991) Correlations between magnetic and superconducting properties of Zn-substituted $YBa_2Cu_3O_{6+x}$. *Phys Rev Lett* 67(22):3140–3143.

30. Uykur E, Tanaka K, Masui T, Miyasaka S, Tajima S (2014) Persistence of the superconducting condensate far above the critical temperature of $YBa_2(Cu,Zn)_3O(y)$ revealed by c-axis optical conductivity measurements for several Zn concentrations and carrier doping levels. *Phys Rev Lett* 112(12):127003.
31. Balédent V, et al. (2011) Evidence for competing magnetic instabilities in underdoped YBa_2 Cu_3 O_{6+x}. *Phys Rev B* 83(10):104504.
32. Matsuzaki T, Momono N, Oda M, Ido M (2004) Electronic specific heat of La_{2-x} Sr_xCuO_4: Pseudogap formation and reduction of the superconducting condensation energy. *J Phys Soc Jpn* 73(8):2232–2238.
33. Bhattacharya S, et al. (1988) Elastic anomalies and phase transitions in high-T_c superconductors. *Phys Rev Lett* 60(12):1181–1184.
34. Wu T, et al. (2013) Emergence of charge order from the vortex state of a high-temperature superconductor. *Nat Commun* 4:2113.
35. Hücker M, et al. (2013) Enhanced charge stripe order of superconducting La_{2-x} Ba_xCuO_4 in a magnetic field. *Phys Rev B* 87(1):014501.
36. LeBouef D, et al. (2013) Thermodynamic phase diagram of static charge order in underdoped YBa_2 Cu_3 O_y. *Nat Phys* 9(2):79–83.
37. Craven RA, Meyer SF (1977) Specific heat and resistivity near the charge-density-wave phase transitions in 2H-$TaSe_2$ and 2H-TaS_2. *Phys Rev B* 16(10):4583–4593.
38. Tabis W, et al. (2014) Charge order and its connection with Fermi-liquid charge transport in a pristine high-T(c) cuprate. *Nat Commun* 5:5875.
39. Shekhter A, Varma CM (2009) Considerations on the symmetry of loop order in cuprates. *Phys Rev B* 80(21):214501.
40. Harris R, et al. (2006) Phenomenology of $\hat{a}$-axis and $\hat{b}$-axis charge dynamics from microwave spectroscopy of highly ordered YBa_2 Cu_3 $O_{6.50}$ and YBa_2 Cu_3 $O_{6.993}$. *Phys Rev B* 74(10):104508.
41. Blackburn E (2014) X-ray diffraction studies of charge density waves in cuprate superconductors: A brief review. *Physica B* 460:132–135.
42. Varma CM (2014) Pseudogap in cuprates in the loop-current ordered state. *J Phys Condens Matter* 26(50):505701.